AD_____

Award Number: DAMD17-02-1-0307

TITLE: Electroacoustic Tissue Imaging

PRINCIPAL INVESTIGATOR: Gerald J. Diebold, Ph.D.

CONTRACTING ORGANIZATION: Brown University
Providence, Rhode Island 02912

REPORT DATE: March 2004

TYPE OF REPORT: Annual

PREPARED FOR: U.S. Army Medical Research and Materiel Command
Fort Detrick, Maryland 21702-5012

DISTRIBUTION STATEMENT: Approved for Public Release;
Distribution Unlimited

The views, opinions and/or findings contained in this report are those of the author(s) and should not be construed as an official Department of the Army position, policy or decision unless so designated by other documentation.

REPORT DOCUMENTATION PAGE

Form Approved
OMB No. 074-0188

1. AGENCY USE ONLY (Leave blank)	2. REPORT DATE	3. REPORT TYPE AND DATES COVERED
	March 2004	Annual (1 Apr 2003 - 31 Mar 2004)

4. TITLE AND SUBTITLE
Electroacoustic Tissue Imaging

5. FUNDING NUMBERS
DAMD17-02-1-0307

6. AUTHOR(S)
Gerald J. Diebold, Ph.D.

7. PERFORMING ORGANIZATION NAME(S) AND ADDRESS(ES)
Brown University
Providence, Rhode Island 02912

E-Mail: gerald_diebold@brown.edu

8. PERFORMING ORGANIZATION REPORT NUMBER

9. SPONSORING / MONITORING AGENCY NAME(S) AND ADDRESS(ES)
U.S. Army Medical Research and Materiel Command
Fort Detrick, Maryland 21702-5012

10. SPONSORING / MONITORING AGENCY REPORT NUMBER

11. SUPPLEMENTARY NOTES

12a. DISTRIBUTION / AVAILABILITY STATEMENT
Approved for Public Release; Distribution Unlimited

12b. DISTRIBUTION CODE

13. ABSTRACT (Maximum 200 Words)

The goal of this research has been to develop new methods of imaging for diagnosing breast cancer. The primary focus of the research, to date, as been on exploring the ultrasonic vibration potential as an imaging method. Research during this period has been on designing and building apparatus, optimizing radio frequency amplification and signal processing schemes, and writing computer programs to store and manipulate data to form images. Theorectical work has been carried out giving a general expression for the vibration potential signal for an object with an arbitrary shape. Experiments have been done on colloidal suspensions to confirm some of the predictions of the theory and to create a several images. Additionally, experiments with phase contrast x-ray imaging have been initiated using a microfocus x-ray tube.

14. SUBJECT TERMS
Vibration potential, ultrasound, phase contrast, imaging

15. NUMBER OF PAGES
13

16. PRICE CODE

17. SECURITY CLASSIFICATION OF REPORT	18. SECURITY CLASSIFICATION OF THIS PAGE	19. SECURITY CLASSIFICATION OF ABSTRACT	20. LIMITATION OF ABSTRACT
Unclassified	Unclassified	Unclassified	Unlimited

Table of Contents

INTRODUCTION

The ultrasonic vibration potential refers to a voltage generated across a pair of electrodes in a solution irradiated with ultrasound. The effect was originally predicted to take place in ionic solutions by Debye[1]. Shortly after its first observation, it was found that large vibration potentials are generated by colloidal suspensions. In a colloid, the effect comes as a result of differential motion of the colloidal particles and the surrounding fluid in response to a mechanical disturbance, which results in a distortion of the normally spherical distribution of charge around the particles. As a result of the differential motion, a dipole is created at the site of each particle, which, when added across a macroscopic distance, gives a potential. The application to tumor detection is based on our observation that a large vibration potential is generated relative to that produced by muscle tissue. Thus, highly vascularized tissue, as is characteristic of the tissue surrounding tumors, should be detectable. It is the contrast mechanism of the vibration potential that is fundamentally differentfrom all other imaging methods that is the distinguishing feature of the method.

Phase contrast x-ray imaging, another method being investigated here, relies on changes in the index of refraction of a body to provide contrast. That is, tissue with differing densities induces different phase lags in the x-rays as they traverse a body. Interference between the different rays gives an intensity modulation to the image. It is important to note that the contrast mechanism for a phase contrast x-ray is totally different from that which produces a conventional x-ray absorption image. In the low spatial frequency limit, for instance, the phase contrast image reproduces the second space derivative of the density in the object. It is important to note that the x-ray source must have a high degree of spatial coherence, which is typically achieved with a synchrotron or a microfocus x-ray tube. Here the production of phase contrast images is being developed using a high power fs laser that is focused to produce a plasma source that approximates a point source.

BODY

The theory of production of the vibration potential has been reviewed by Povey[2], Zana and Yeager[3], Babchin, Chow and Sawatzky,[4] and O'Brien, Cannon, and Rowlands[5-8]. The theory that we employ, and that which is generally accepted, is that of O'Brien and coworkers[5-8]. According to O'Brien's theory, the magnitude of the vibration potential generated in a colloidal suspension is proportional to the density difference between the particle and the fluid, the volume fraction of the particles, the dynamic mobility of the particle, the inverse of the conductivity, and the magnitude of the ultrasonic velocity, which depends on the sound intensity. Since the idea of vibration potential imaging is new, a goal of the research is to give a rigorous theory that explains how the geometry of irradiation determines the vibration potential in time. As described below, a theory has been developed for the generation of the vibration potential signal for the case where ultrasound is propagated normal to two grounded plates between which is the body under study. The assumption of grounded plates would be approximated in the

laboratory by connecting a low input impedance amplifier between the plates, as is planned in experiments here.

The work with phase contrast imaging, begun only recently, has focused on setting up a laboratory provided with a microfocus x-ray tube, a liquid nitrogen cooled CCD camera, a phosphor screen, optics, and sample mounts. The apparatus is interfaced with a computer so that the x-ray tube can be turned on and off remotely, and the CCD image transferred to the computer for storage. Preliminary experiments have been carried out showing that the microfocus tube is capable of generating a beam of x-rays sufficiently coherent that phase contrast images can be made.

KEY RESEARCH ACCOMPLISHMENTS

The theory of production of a vibration potential image for one experimental arrangement has been formulated. The theory is quite long, so only a synopsis of the main features of the theory is given here. The starting point for the theory is O'Brien's expression for the electric field E generated by the gradient of the pressure p,

$$\mathbf{E} = \frac{f \Delta \rho_m \mu_E}{\rho_m \sigma^*} \nabla p, \qquad (1)$$

where f is the volume fraction of colloidal particles in the fluid, μ is the electrophoretic mobility of the particles, ρ is the mass density of the suspension, and $\Delta\rho$ is the difference in densities between the particles and the surrounding fluid, and σ^* is the complex conductivity. The material in the body is considered to be both a dielectric with dielectric constant ε and a weak conductor with a conductivity σ^*. Although the body is composed of an object that is considered to be colloidal or ionic so that it generates a vibration potential, the object and body are considered to have uniform properties so that both are considered to have conductivity σ^* and a dielectric constant ε . The geometrical arrangement for the problem to be solved is shown in Fig. 1. A beam of ultrasound is directed from below the lower electrode normal to the electrode surface. On traversing the object, the ultrasound produced a vibration potential, which is conveyed to the electrodes by two mechanisms. The first is through the production of a polarization on the surface of the object, which induces charge of opposite polarity to appear on each electrode. Since the electrodes are connected through a virtual short circuit, a positive charge can appear on one electrode and a negative charge on the other. The second mechanism comes as a result of the finite conductivity of the body. Here, the field that is induced in the body as a result of vibration potential cuts the metallic conductors producing a current. The resulting current that is induced by the field appears partly in the external circuit. Note that the circuit is considered to be a short circuit. This assumption was made in order to have the potential on each electrode zero so that the problem could be solved in a straightforward manner. In fact, such a circuit is approximated by placing a low input impedance amplifier in the circuit between the electrodes, and which is planned for experimentation. The other approximation that would result in a soluble electromagnetic problem would be the approximation of an open circuit, as would be realized in the laboratory with a high input impedance preamplifier.

The critical step in solving the problem is to consider the displacement vector **D** as arising from both an acoustically generated polarization $\mathbf{P}_a$, and the electric field **E** through the relation

$$\mathbf{D} = \varepsilon\mathbf{E} + \mathbf{P}_a, \tag{2}$$

Substitution of Eq. (2) into Maxwell's equations, used in the quasistatic approximation, with

$$\mathbf{E} = -\nabla\phi. \tag{3}$$

whrere φ is a potential, and

$$\mathbf{P}_a = \alpha(\omega)\nabla p \tag{4}$$

where

$$\alpha(\mathbf{x},\omega) = \varepsilon\, f\, \Delta\rho_m\, \mu_E / \rho_m \sigma^*,$$

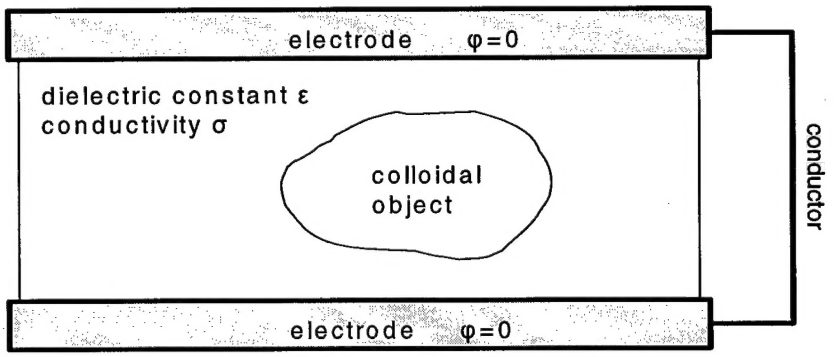

Figure 1. Schematic diagram of the geometry for vibration potential imaging. Ultrasound enters from below the electrode and propagates upward, normal to the surface to the electrode.

gives a time domain partial differential equation for the potential

$$\sigma\nabla^2\phi + \varepsilon\frac{\partial}{\partial t}\nabla^2\phi = \frac{\partial}{\partial t}(\nabla\cdot\mathbf{P}_a) \tag{5}$$

It can be seen that the source term on the right hand side that generates the potential depends on the time derivative of the divergence of the polarization generated by the ultrasound. It is also noteworthy that if the conductivity is zero, then a first integral of Eq. (5) is Poisson's equation with $\nabla \cdot P_a$ representing a charge density. If the conductivity is large, so that the second term is small, then the time derivative of the divergence of the polarization becomes important.

Since most experiments are conducted with sinusoidal acoustic waves, it is not difficult to show that the frequency domain potential is

$$\nabla^2 \tilde{\phi} = \nabla \cdot (\alpha^{\dagger} \nabla \tilde{p}) \ , \tag{6}$$

where $\alpha^{\dagger}$ is given by

$$\alpha^{\dagger}(\mathbf{x}, \omega) = \frac{i\omega}{\sigma + i\omega\varepsilon} \alpha(\mathbf{x}, \omega) \ .$$

It is next required to solve Eq. 6 for the geometry at hand, where the potential on the electrodes is zero, and where the electrodes can be considered to be infinite in the x and y directions. The method of solution of Eq. 6 taken here is to find a Green's function for the two plates, which when integrated over according to Green's theorem gives the potential. The derivation of the Green's function for the geometry chosen gives the Dirichelet Green's function as

$$G_D(\mathbf{x}, \mathbf{x}') = -\frac{1}{2\pi^2 h} \sum_{1}^{\infty} \sin(\frac{m\pi}{h} z) \sin(\frac{m\pi}{h} z') \iint_{-\infty-\infty}^{\infty\infty} \frac{e^{i\kappa_x (x-x') + i\kappa_y (y=y')}}{[(\frac{m\pi}{h})^2 + \kappa_x^2 + \kappa_y^2]} d\kappa_x d\kappa_y . \tag{7}$$

Since the potential on the electrodes is zero, and the Green's function by design is zero on the electrodes as well, the potential at any point in space between the electrodes is given by

$$\tilde{\phi}(\mathbf{x}) = \int_{V'} G_D(\mathbf{x}, \mathbf{x}') \nabla' \cdot [\alpha^{\dagger}(\mathbf{x}', \omega) \nabla' \tilde{p}(\mathbf{x}')] dV', \tag{8}$$

According to the discussion above, there are two mechanisms for production of current in the circuit. In the first mechanism there is a time varying displacement in the dielectric so that a current $\mathbf{J}_P = \partial \mathbf{D} / \partial t$ is produced. The displacement vector is found from the electric field through $\mathbf{D} = \varepsilon \mathbf{E}$, where the field is found as the gradient of the potential as in Eq. 3. In the second mechanism, the presence of an electric field provides a driving force for a current composed of free charges, where the current density $\mathbf{J}_F$ is given by $\mathbf{J}_F = \sigma \mathbf{E}$. It follows then that $\mathbf{J}_P$ and $\mathbf{J}_F$ are given by

$$\mathbf{J}_P(\mathbf{x}) = -\varepsilon \frac{\partial}{\partial t} \nabla \tilde{\phi}(\mathbf{x}). \tag{9}$$

and

$$\mathbf{J}_F(\mathbf{x}) = -\sigma\nabla\tilde{\phi}(\mathbf{x}). \tag{10}$$

The total current density is the sum of $\mathbf{J}_P$ and $\mathbf{J}_F$. The current in the electrodes I is the integral of the two current densities over the x and y coordinates,

$$I = \frac{(\sigma + i\omega\varepsilon)}{2\pi^2 h}\iint_{s'} dx\,dy\int_{V'}\frac{\partial}{\partial z}G_D(\mathbf{x},\mathbf{x}')|_{z=0}\nabla'\cdot[\alpha^{\dagger}(\mathbf{x}',\omega)\nabla'\tilde{p}(\mathbf{x}')]dV' \tag{11}$$

The integration over x and y gives two delta functions and the resulting expression can be summed to give I as

$$I = \frac{i\omega}{h}\int_V \alpha(\mathbf{x},\omega)\frac{\partial}{\partial z}p(\mathbf{x})\,dx\,dy\,dz. \tag{12}$$

Integration of this expression by parts yields a second expression for the current,

$$I = -\frac{i\omega}{h}\int_V [\nabla\alpha(\mathbf{x},\omega)]_z p(\mathbf{x})\,dx\,dy\,dz. \tag{13}$$

It is evident that the gradient of the concentration of the spatial distribution of the colloidal

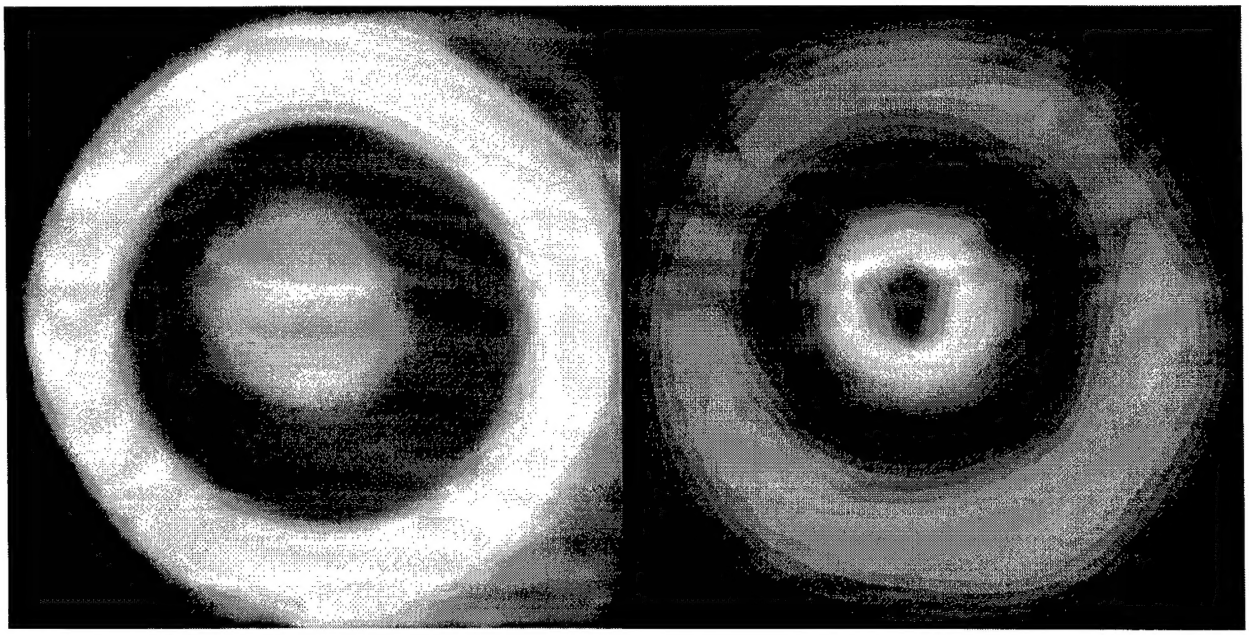

Figure 2. Left: photograph, and right vibration potential image of a colloidal phantom cast in agarose.

object parallel to the direction of propagation of the pressure wave integrated over the pressure gives the current in the circuit. From this general expression, simpler expressions can be obtained for the current in a one-dimensional geometry. In addition, simple expressions for the current can be found for objects such as a sphere, cylinder, or a layer where the integration can be carried out to give a closed form expression. In more complicated cases, numerical integration of the general expression can be carried out. In terms of using the vibration potential as a diagnostic, it would be desirable to be able to invert the expressions for the current so as to yield the spatial distribution of colloid directly. This problem will be attacked in the future.

We have succeeded in obtaining what might be called "surface" images of colloidal objects cast in an agarose block. The image shown in Fig. 2 is a disk surrounded by a ring of colloidal material in agarose. The vibration potential signal was produced by rastering a 1 MHz pulsed ultrasonic beam across the phantom. The image is an amplitude image, in the sense that only the amplitude of the vibration potential was recorded, and not the arrival time of the signal or other frequency dependent information. The image shown in Fig. 3, also taken with 1 MHz focused radiation uses time of arrival to give a third dimension. Again, the image is an amplitude image, where a predetermined amplitude is used as a cutoff for registering a 1 or a 0, and the position along the z axis is determined by the arrival time of the vibration potential signal relative to the launching of the acoustic burst.

We have succeeded in obtaining images of small objects using a microfocus x-ray tube. The goal of this work is to use the small spot size of the laser source for producing phase contrast images of tumors. The term "phase contrast" imaging[9, 10] refers to methods that may be considered as arising from interference in the phases of x-rays that travel different paths to the detector. The method requires spatial coherence in the x-ray source, as is obtained from

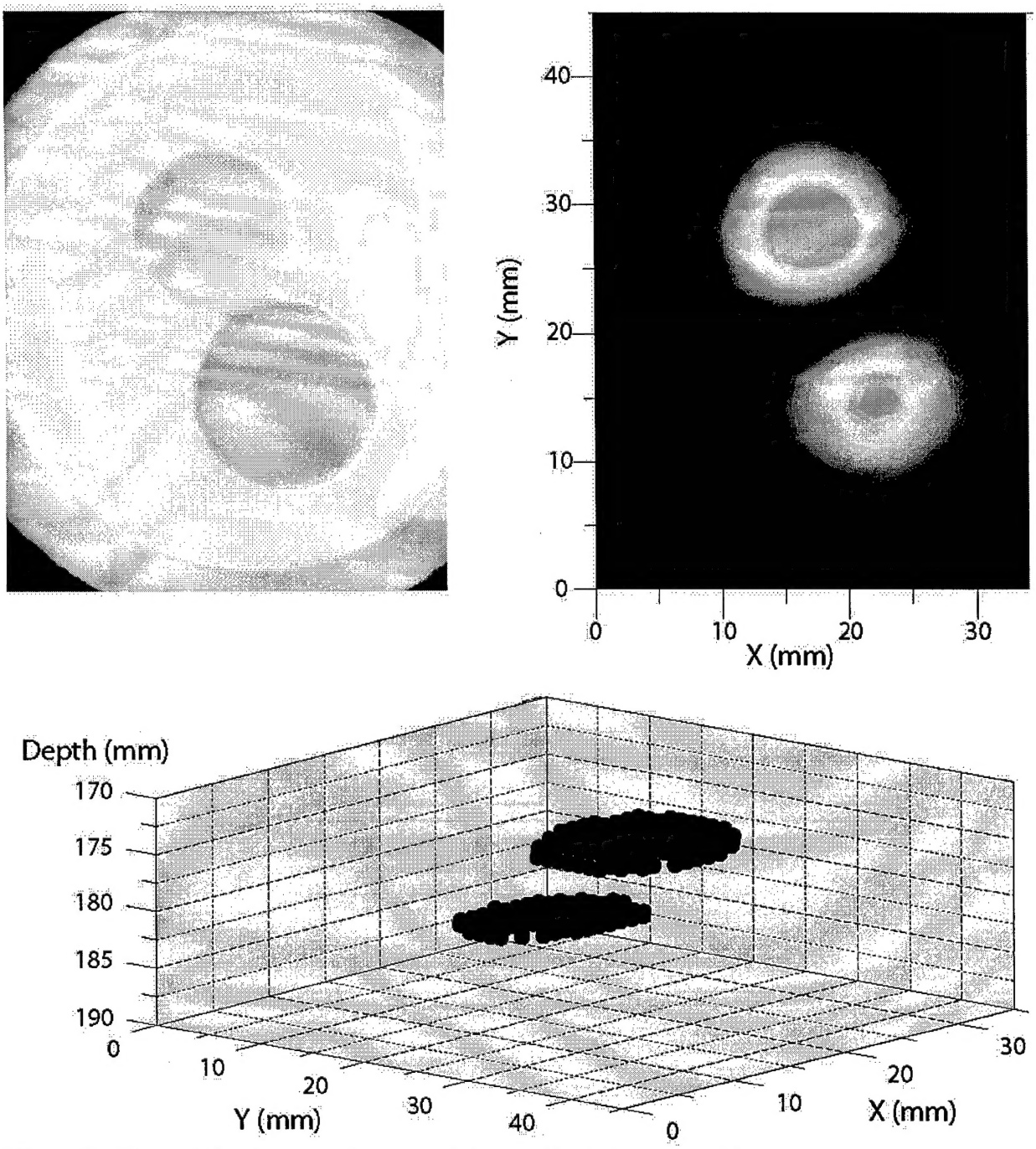

Figure 3. Upper left, photograph; upper right amplitude image; and bottom,

synchrotrons or sources that approximate point sources. The theory of the image formation predicts that in one regime of operation, dependent on the spatial frequencies in the object, the wavelength of the x-ray and the distances of the source-to-object and object-to-image planes that

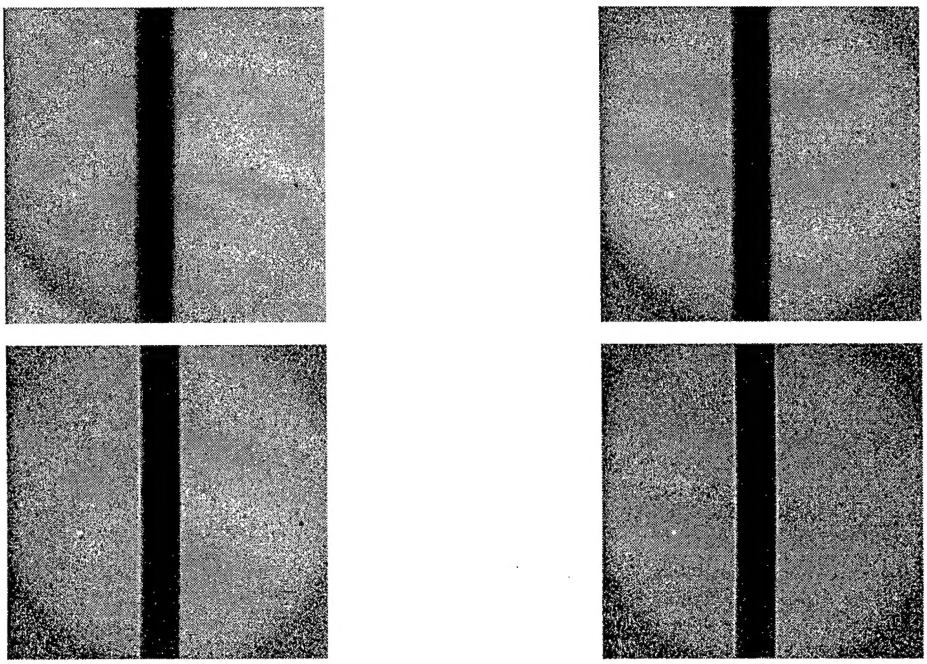

Figure 4. Phase contrast images of a 300 micron nylon fiber taken at x-ray tube voltages of upper left, 20; upper right, 50; lower left 70; and lower right, 90 keV.

the image, in addition to the shadow formed by absorption will have a component of the image proportional to the second derivative of the phase of the object. It is possible to cast the theory in terms of the density of the image, in which case, the image has component proportional to the second derivative of the density. The phase contrast image thus heightens boundaries. The x-ray images of a section of 300 micron diameter nylon fiber shown in Fig. 4 show phase contrast to varying degrees depending on tube voltage. The image taken with the highest voltage shows the dark absorption profile of the fiber, but, in addition, shows a light area around the edges of the fiber that is essentially the phase contrast component of the image resulting from phase changes in the x-rays traversing the fiber. An alternate way of looking at phase contrast imaging is that the x-rays are deflected as they traverse the object. The light line parallel to the fiber in Fig. 4 represents the effect of refraction of x-rays outwardly from the fiber. The different degrees of phase contrast in the four images is dependent on the focusing characteristics of the tube—the higher the voltage on the microfocus tube used here, the smaller the x-ray point spread function.

KEY RESEARCH ACCOMPLISHMENTS

The most important advance in the research on vibration potential imaging has been the formulation of a rigorous theory for imaging. The result of this theory can be applied to model

simple objects such as a spherical body, a cylindrical body, and a layer. The theory for a layer provides a basis for imaging in one dimension. The theory gives an integral which can be used for any arbitrary shape object. As well, the theoretical results provide the fundamental integral for production of the observable in the experiment, which is the current, and hence inversion methods can be explored that determine profiles of the object from data.

An apparatus has been assembled so that images can be made using the vibration potential. Amplification and signal processing methods have been worked out so that the time of arrival of the vibration potential signal, and its phase and amplitude can be recorded on every firing of the ultrasonic transducer. Images have been obtained of colloidal phantoms that are based on a one-dimensional model for image formation. Computer programs for processing and plotting data have been written. At this point the sophistication of the imaging method has advanced so that images are publishable as are the principles of vibration potential imaging.

X-ray phase contrast images have been obtained using a microfocus x-ray tube. The laser x-ray source has been tested in a primitive experiment. Further development of the target and focusing optics is under way.

REPORTABLE OUTCOMES

The principle of vibration potential imaging will be published shortly when all the details of the mathematics are complete. Acceptable, but by no means optimized, electronic amplification and signal processing schemes have been worked out and will be published. Surface images of phantoms have been taken and will be reported.

CONCLUSIONS

The method of imaging based on the vibration potential has been established. Although only a one-dimensional imaging scheme has been tested in the laboratory, the method has been shown to give realizable images. The theory of vibration potential imaging has been given for an arbitrary object. This theory will for the basis for future, more complicated image acquisition schemes. Phase contrast images using a microfocus tube have been made. Investigation of the use of the pulsed laser method, which, in principle, should give a high resolution image are in progress.

REFERENCES

1. P. Debye, "A Method for the Determination of the Mass of Electrolytic Ions", J. Chem. Phys. 1, 13 (1933)
2. M. J. Povey, *Ultrasonic Techniques for Fluids Characterization* (Academic Press, San Diego, 1997) See Ch. 5.1.5.7, p 150
3. R. Zana and E. Yeager in "Modern Aspects of Electrochemistry" Vol. 14 (Plenum, New York, 1982), J. Bockris, B. Conway and R. White, eds.
4. A. J. Babchin, R. S. Chow and R. P. Sawatzky, "Electrokinetic Measurements by Electroacoustical Methods", Adv. in Colloid and Interface Sci. 111, 30, (1989)

5. R. W. O'Brien, D. W. Cannon, and W. N. Rowlands, J. Colloid and Interface Sci.173, 406 (1995);
6. R. W. O'Brien, Applied Mathematics Preprint, AM86/25 Univ. South Wales, 1985;
7. R. W. O'Brien, J. Fluid Mech.190, 71 (1988); R. W. O'Brien, J. Fluid Mech.212, 81 (1990);
8. R. W. O'Brien, P. Garside, and R. J. Hunter, Langmuir 10, 931 (1994)
9. S. W. Wilkins, T. E. Gureyev, D. Gao, A. Pogany, and A. W. Stevenson, Nature 28, 384 (1996)
10. A. Snigirev, and I. Snigireva, Rev. Sci. Instrum. 66, 5486 (1995)

APPENDIX

No appendix is necessary